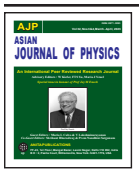

Asian Journal of Physics
Vol. 32, Nos 3 & 4 (2023) 149-158
Available on: www.asianjournalofphysics.com

ap

Experimental determination of the MTF of a diffraction limited image forming system: an approximation to the eye pupil characterization

Elena Alonso-Redondo[1], Maria L Calvo[1], and Vasudevan Lakshminarayanan[2]

[1]*Department of Optics, Faculty of Physical Sciences, Complutense University of Madrid, 28040 Madrid, Spain*

[2]*School of Optometry and Vision Science and Department of Physics and Electrical and Computing Engineering, University of Waterloo, Waterloo, ON, Canada N2L3G1*

Dedicated to Prof Jay M Enoch

We present results on the design of an optical image forming system. The design will enable us to study small apertures effect in image formation of the eye. The system is designed to operate with various laser sources and to obtain the Modulation transfer function (MTF) dependence with wavelength. It is then extended to characterize the monochromatic MTF function, its spatial dependence on the aperture size of the limited system and the spectral dependence of the optical system response. Computational work is compared with experimental data.

Keywords: Diffraction, Image processing optical systems, Modulation transfer function, Eye pupil.

1 Introduction

The fundamentals of image treatment, analysis and design of optical systems for image acquisition and processing are nowadays quite well established subjects with wide applications in many areas of physics, optics, biomedicine and, in general, in optical information processing. Since the very early work of J Goodman [1], A B Van der Lugt [2] and others, the vast number of publications, for several decades, reflects the fact that this subject is currently introduced as a basic topic in many courses on fundamental and specialized courses in optics. In addition, the introduction of Fourier analysis by P M Duffieux [3] as early as in 1946 gave rise to Fourier optics as a powerful branch in physics and engineering.

In the context of vision science, the applications of image processing and Fourier optics to the study of the human eye as a hybrid optical-neural processor, has helped in understanding the complex mechanisms of information processing inherent to visual processing.

In this regard one of the purposes in the present study is to characterize and evaluate the performance of an optical experimental setup aimed to design and determine some particular functions. These functions are related to the quality of the response of an optical system. In particular, one can study Modulation Transfer Functions (MTFs) of an optical system limited by diffraction, which is the modulus of the complex Optical Transfer Function (OTF).

The MTF provides a measure of the quality of an optical system as well as information about the spatial frequency range processed by the system [1]. Moreover, MTF allows us to estimate parameters, namely: contrast, cut-off frequency or optical resolution capability. In particular, these functions are of key importance in imaging systems and can be applied to visual processing. In a pioneering work, in 1972

Corresponding author
e mail: mlcalvo@ucm.es (Maria L Calvo)

Jay Enoch and collaborators studied the experimental MTF of isolated human central foveas. From their obtained results it was shown that well oriented retina photoreceptors have associated with well-defined MTF functions and provided precise data on cut-off frequency as a general behavior for vertebrates and HVS [4].

In this work MTF with a compound optical system, that simulates approximately the optical section of Human Visual System (HVS), will be obtained. The response is studied with an object as a Foucault test. We also analyze the effect of a finite pupil size, geometry as well as the light wavelength. Comparative studies are discussed in some cases.

The paper is structured as follows. Section 1 is dedicated to introduction. In Sec 2 the analytical OTF is derived and its relation to MTF and contrast is given. Also, OTF is calculated for the particular case of a circular pupil using a convenient computational software. In Sec 3 the optical section of the human eye is presented as an optical image forming system. Thereafter MTF for each section of the optical part of the human visual system is provided. In Sec 4 the experimental setup and method for MTF calculation is presented. Finally, results are presented in Sec 5 with discussion and conclusions in Sec 6.

2 Fundamentals: OTF and MTF of a diffraction limited image forming system

The key equation to study OTF is the diffraction integral [5]:

$$U(x', y') = \hat{C} \iint G(x, y)\, exp\{i2\pi(xx' + yy')\}dx\,dy \tag{1}$$

In Eq (1) and for a fixed axial distance z_0, $U(x', y')$ denotes the complex amplitude distribution of light scalar field after propagating in free space. Here $\hat{C}$ is a complex constant and $G(x, y)$ is the pupil function of the system. Primed coordinates indicate image space, whereas unprimed stand for object space. The aperture pupil is expressed as:

$$G(x, y) = \begin{cases} |G(x, y)|\, exp\{-iknW(x, y)\}, & (x^2 + y^2) \le R \\ 0, & (x^2 + y^2) > R \end{cases} \tag{2}$$

In Eq (2), R is the aperture radius, and $W(x, y)$ the aberration function, which is zero for a perfect, aberration-free system. The intensity, $B(x', y')$ at the image plane (output of the system) is the square modulus of $U(x', y')$. Its direct Fourier transform is denoted by $b(u, v)$, where (u, v) are the spatial frequencies of the system. According to the properties of the Fourier transform:

$$b(u, v) = \int\int_{-\infty}^{\infty} G(x, y) \cdot G^*(x - u, y - v)\, dx\, dy \tag{3}$$

In Eq (3) G^* is the conjugate of the complex pupil function, where for simplicity, we have considered $\hat{C} = 1$ and symmetry properties for the aperture. Equation (3) matches with the autocorrelation of the pupil function $G(x, y)$. If we consider the pupil function as a circle of radius R, then the OTF has the profile as displayed in Fig 1 and represents the diffraction limit of the system.

Generally, OTF is described by a complex function due to the presence of aberrations at the aperture. Then, OTF consists of the product of the magnitude and the complex phase function. The OTF magnitude is the MTF. Phase function is important in highly aberrated systems or in the case of Human Visual System (HVS), for large angles or eccentric apertures.

The term contrast is frequently used in discussions about optics, photography and vision. It is defined as

$$C = \frac{W_{max} - W_{min}}{W_{max} + W_{min}} \tag{4}$$

where W_{max} stands for maximum energy flux density and W_{min} stands for minimum energy flux density at the image or detection plane. Usually, this quantity also called Michelson contrast is expressed as a percentage. When a sinusoidal field with well-defined spatial frequency is transmitted through an optical system, it is

possible to measure W_{max} and W_{min} at the image or detection (output) plane and obtain contrast C for that spatial frequency. In a given optical system, C is a function of spatial frequency giving the behavior of the MTF. Figure 1 displays the characteristic representation of the MTF for an ideal perfect optical system.

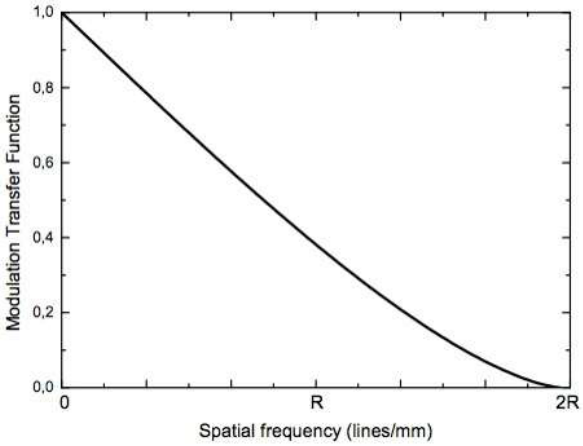

Fig 1. Modulus of the autocorrelation of a circle pupil function (See Eq (3)). This function is identically perfect OTF for a system free from aberrations and only affected by diffraction [1].

3 The human eye system and its MTF

As a general definition, the eye is a specialized light-sensitive sensory structure of animals that in nearly all vertebrates, most arthropods, and some mollusks is the image-forming organ of sight. In particular, the human eye can be considered as a living neuro-optical device. Therefore, can be characterized by specific OTF, MTF and spatial and temporal frequency range responses.

In order to model the morphology of the eye to be applied later for the purpose of our study, some complementary measurements were performed by using a biometric interferometer Lenstar LS900 (Haag-Streit, Switzerland). The measurements were performed on 9 healthy adult subjects in both eyes (see Table 1). The eye shape is approximately spherical and has an average diameter, in emmetropes, of 24.54 mm. The lens thickness of the relaxed human eye is 3.91 mm, but may vary during accomodation of the eye. The iris forms the aperture stop of the eye. The mean mesopic, photopic and dilated pupil diameter is: 6.37±0.89, 4.06±0.70 and 7.58±0.82 mm, respectively [6].

This aperture stop is known as the pupil and has an average diameter of 5.11 mm under scotopic illumination. The pupil size is determined by the sphincter and dilator muscles, which are under autonomic control (reflex). Some of the factors affecting the pupil size of HVS are: level of illumination, accommodation, psychological factors or age [7]. We do not consider these factors in the current study.

Table 1. Average biometric data of 18 healthy eyes (9 subjects)

	Mean value(mm)	SD(mm)
Axial length	24.54	1.23
Lens thickness	3.91	0.27
Pupil diameter	5.11	1.03
Corneal diameter	12.38	0.31

To introduce a simplified model of the HVS, one can consider the optical system of the human eye as a photographic camera in the initial stages. Light passes through the iris diaphragm. After iris, the

crystalline lens forms in the anterior portion of the retina an inverted focused image. Photoreceptors of the retina confine light and after a complex biochemical process transduce the incident light energy into a neural signal. The MTF can be defined for different parts of HVS: cornea plus lens, retina, retina plus neural system, and isolated neural system. Figure 2 shows the MTFs for each part, including the isolated retina. As suggested in Fig 2, the ratio between the MTF for retina + neural system (C) and the MTF for isolated retina (A) provides isolated neural response. Assuming, as an approximation, HVS a linear system [8], there is a global MTF response defined by the product of the MTFs of each part as:

$$MTF_{total} = MTF_{cornea+lens}\, X\, MTF_{retina}\, X\, MTF_{neural} \tag{5}$$

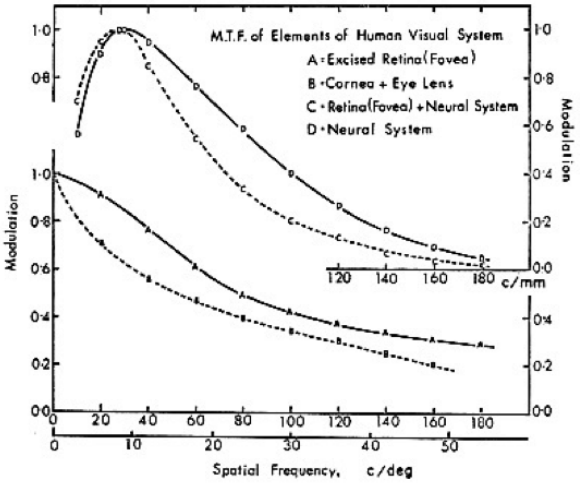

Fig 2. Experimental MTF curves for different parts of human visual system. Curve A represents MTF for isolated retina (corresponding to the fovea). Curve B provides MTF of cornea and lens acting together. Curve C is the MTF determined by interferometric methods and representing the human retina plus neural response. Curve D = C/A is digitally manipulated in order to obtain an estimation of the form of human neural response. (Source: Fig 5 from Ref [4]).

In Fig 2, the spatial frequency range is also given in terms of cycles/deg for vision measurements. It gives a cut-off frequency near 180 cycles/deg. We notice that the obtained low-frequency peak, as it was earlier observed by Campbell and Green [9] is formed due to the neural processing system and not necessarily by the retina itself. The total behavior is a result of the multiplicative operations as stated in Eq (5). In the present study, we have obtained the MTF of an optical system simulating the optical part of the HVS. It includes the lens, and the retina and the neural response is not considered. Thus the expected shape of our measured MTF may be rather similar to the curves A and B of Fig 2. Note that MTFs which include neural system, as curves C and D, have a distinct behavior associated with the performance of a band-pass filter [10].

4 Experimental setup

The purpose of the experimental set-up is to simulate the optical section of a human eye (pupil, lens, and eye movements) and to obtain the related experimental MTF functions. First, we stress that the quality and characteristics of the different eye optical components and the combination, operating conjunctly, are described in terms of: cornea, pupil, lens, accommodation, scattering, aberrations, retina, resolution and focal length, depth of focus and refractive errors. According to the experimental set-up, we have implemented a system representing an artificial eye corrected from aberrations by using aberration free lenses. All individual

characteristics namely: scattering, depth of focus and refractive errors are obviously not implemented. We may notice that the biological optics of the human eye reveal local irregularities that are not present in man-made optics such as the mentioned internal scattering [11].

In order to analyze the pupillary effect the experimental arrangement comprises a variable aperture, a lens, a rotating diffuser and a CCD camera. These components have been used to simulate iris, eye lens, the vitreous and the detection system. Since our artificial eye is 300 mm long, the scale factor for the experimental arrangement is 12,2. The whole set-up is shown in Fig 3. It consists of a laser source, pinhole P1, attenuator A, collimating lens L1, beam expander L2+L3, object O which is a standard line pair patterns (1951 USAF Resolution Target). After the object a dynamic diffuser D is placed. It consists of a circular transparent semi-rigid plastic sheet attached to a 12 V electrical motor placed near the CCD camera, and acts as a rotating diffuser during the measurement process. The role of the rotating diffuser is to create a dynamic image simulating eye movements at the image formation process [12,13]. The size of pixels of the CCD camera (Sony, California) is 4.65 µm.

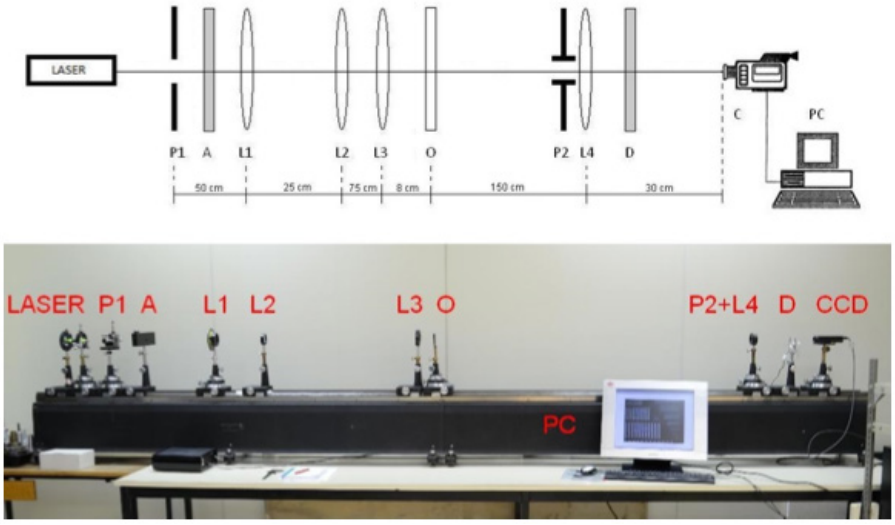

Fig 3. Arrangement of the experimental setup (top). Photograph of the system (bottom). Laser source; P1: Pin-hole (25µm); A: Attenuator; L1: Collimating lens; L2-L3: Beam expander; O: Object (test); P2: Variable diaphragm integrally mounted with lens L4; L4: Converging lens. D: Diffuser. CCD: Camera. PC: Computer.

In order to study the MTF dependence with source wavelength various alternative light sources have been used in this experiment, as: i) a He-Ne and semiconductor lasers with wavelengths 632.8 nm and 635 nm, respectively, ii) three laser pointers with 655, 532 and 402 nm wavelengths, respectively. The coherence of the sources has been considered since it affects the image formation and resolution according to Eq (5) [14-16]. The semiconductor laser and the laser pointers have a lower degree of coherence than He-Ne laser as expected [17].

5 Results and discussion

Following the experimental procedure detailed in the previous section many results have been achieved. First, the influence of the dynamic diffuser in image formation quality has been evaluated through the MTF characterization. Secondly, a study on finite pupil size as a variable has been explored. Third, the effect of wavelength on the MTF has been revealed. Finally, we compared the MTFs for light sources with

varying degrees of coherence and with the perfect MTF. The applied method to obtain the MTF curves is based upon the measurement of contrast factor (Eq (5)) for each group of bars of a standard test (1951 USAF Test Target). In order to obtain measurements of contrast a specific computing program was developed in MatLab (Mathworks Inc., Massachusetts). Care has been taken for ensuring a uniform background illumination in the optical system since it directly alters the contrast measurements.

5.1. Dynamic Diffuser

As indicated before, the role of the rotating diffuser is to simulate eye movements [13]. The MTFs of the optical system operating with and without this rotating diffuser were obtained. As the light source, a He-Ne laser was used and a variable pupil (diaphragm) with a maximum aperture of 29.5 mm was located in front of the lens. In Fig 4, it is shown how the placement of the diffuser into the artificial eye modifies the MTF curve. Moreover, the rotating diffuser induces the formation of a dynamic image projected on the camera. We notice that this dynamic device causes breaking the temporal coherence in the experiment as a result of temporal decorrelation. This makes the contrast at high frequencies to experience a decrease with respect to the MTF results without diffuser. The spatial frequency cut-off is 12.5 ± 0.3 lines/mm for the system operating without diffuser. The inclusion of the same reduces the cut-off frequency to a value of the order of 10.0 lines/mm.

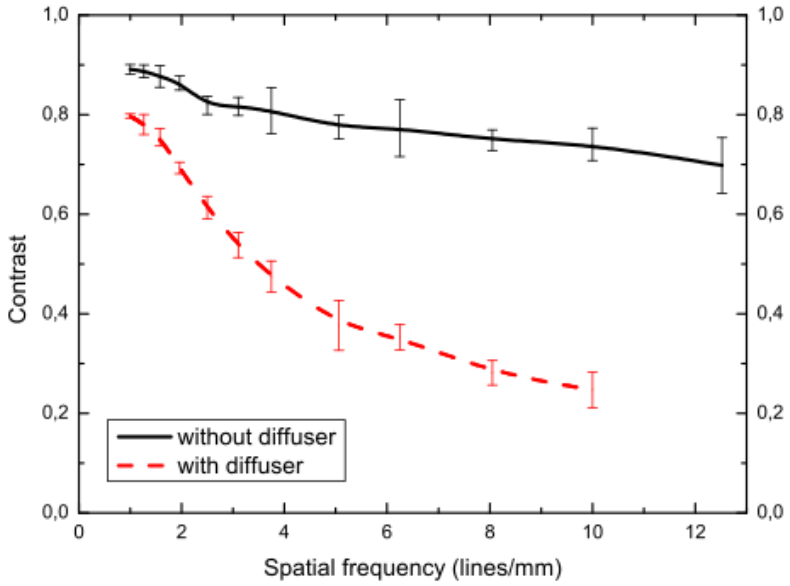

Fig 4. MTF curves for an optical system with a He-Ne laser source (632.8 nm) and a pupil size of 29.5 mm for two cases: with rotating diffuser (dashed line); without diffuser (solid line), and dispersion error bars (2 SD).

5.2. Pupil size

To evaluate how the finite pupil size influences the MTF curves, eight different pupil diameters ranging from 29.5 to 11.0 mm were used (Fig 5).

A He-Ne laser source illuminated the system and the dynamic diffuser was operating, as well. The contrast values strictly decrease as spatial frequency increases, as expected. Any specific behavior of the MTFs as a function of pupil size cannot be revealed from Fig 5. It is noticeable the dispersion of error bars. The higher the spatial frequency the larger the dispersion error bar. This has been attributed to several different factors. First, the rotating diffuser forms a dynamic image in front of the camera, which for certain frequencies, is not detectable due to low contrast, therefore affecting the dispersion of the contrast values.

Secondly, a perfect uniform background illumination is not achievable. Minor imperfections in optical devices of the set-up contribute to generate particular diffraction patterns having a direct impact on contrast measurements. Thirdly, since the light beam is partially coherent, Talbot sub images appear blurring the primary images of the test as a consequence of the periodical structure of the object [18]. Fourth, when partially coherent light is used, images defocused out of image plane and contrast inversion occurs. All of the mentioned facts contribute to a high standard deviation at high frequencies.

There is an alternative procedure to assess pupil size effect by MTF measurement. On the underlying theory of optical design system, in general, the merit function provides a useful tool to quantify the transfer of information and image quality [1]. Moreover, the merit function provides information on the accordance between experimental data and the model for a particular choice of parameters. In this paper, the merit function is defined as the area between MTF curves for maximum and minimum pupil size:

$$M = \int_{u_0}^{u_c} [MTF_1(u) - MTF_2(u)]du \tag{6}$$

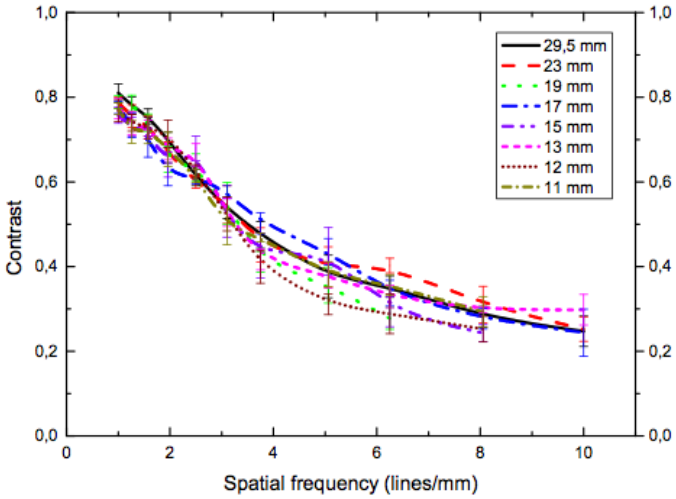

Fig 5. Average MTFs and dispersion error bars (2 SD) for eight different pupil diameters values ranging from 29.5 mm to 11.0 mm. See text for details.

In Eq (6) integration limits denote the interval (u_0, u_c) corresponding to lowest and highest spatial frequencies processed by the system. MTF_1 and MTF_2 represent two particular *MTFs* for two pupil sizes, respectively. As a rule for interpreting the results, the smaller the area the more optimized the performance for the system. MTFs have been adjusted to an empirical exponential function [19]:

$$MTF(u) = y_0 + A\ exp[-u/u_1] \tag{7}$$

In Eq (7), y_0, A and u_1 are fitting parameters obtained by software OriginPro (OriginLab, Massachusetts). The merit function M was obtained for various setups with laser sources He-Ne, semiconductor laser and laser pointer, respectively. A smaller M was obtained in the case of He-Ne laser, followed by the semiconductor and the laser pointer (see Table 2). Therefore, it can be stated that optical resolution is better for the system in the case of a He-Ne laser source operation. The semiconductor laser provides another source characteristic in addition to He-Ne and laser pointer and allows a comparative study for contrast values.

Table 2. Merit function for three setups with three alternative laser sources

Merit function(units^2)	He-Ne	Semiconductor	Pointer
M	0.03	0.57	0.92

5.3 MTF as a function of wavelength

In order to explore the behavior of MTF as a function of source wavelength a comparative study is presented. Figure 6 exhibits the performance of contrast as a function of spatial frequency and pupil size for three wavelength values considered: red ($\lambda = 655$ nm); green ($\lambda = 532$ nm) and blue ($\lambda = 402$ nm). It can be noticed that for lower frequencies and larger pupil diameters (Fig 6 a, b) the contrast is almost similar for all wavelengths considered. Moreover, for higher frequencies and smaller pupils (Fig 6 c, d) the spectral dependence is more noticeable. The contrast differs markedly between curves of different colors, being always greater for the blue case and lower for the green or red. According to spatial frequency wavelength dependence: $u = x/\lambda f$, where x is the spatial coordinate, f is the focal length, and λ is the source wavelength, the highest contrast is obtained for the blue light source. Moreover, contrast values are higher for larger pupil sizes. A similar behavior was also observed for all the three wavelength values considered and for fixed spatial frequency.

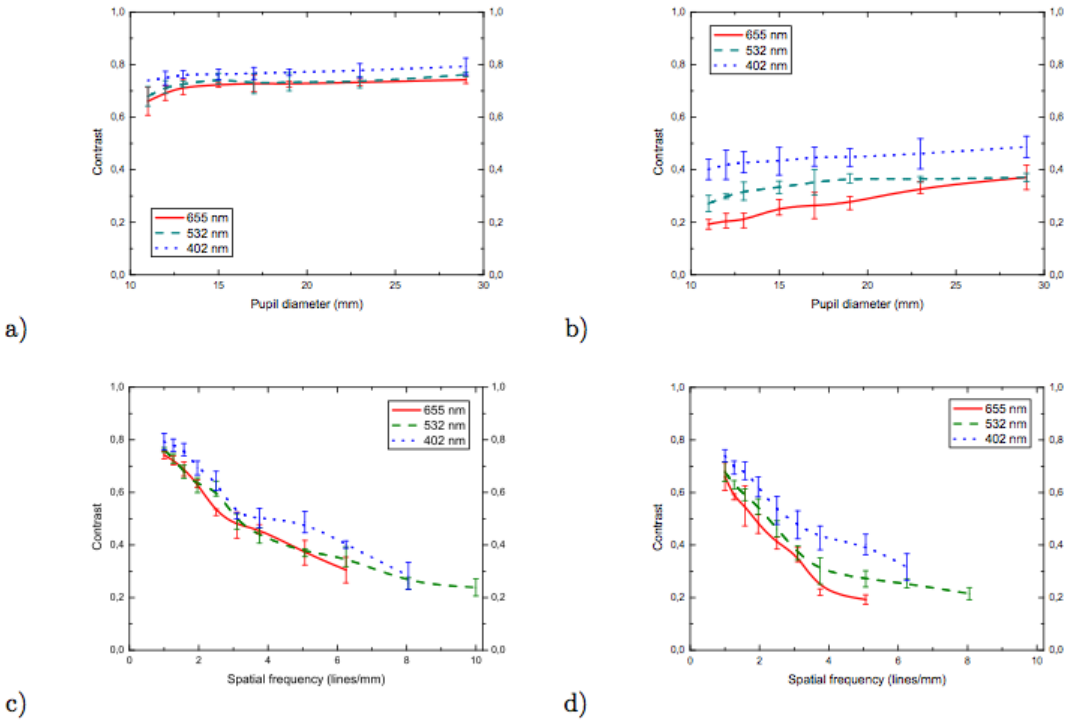

Fig 6. (a) Contrast as a function of pupil size and fixed spatial frequency: 1 line/mm. (b) Contrast as a function of pupil size and fixed spatial frequency: 5 lines/mm. (c) Contrast as a function of spatial frequency and fixed pupil size: 29.5 mm diameter. (d) Contrast as a function of spatial frequency and fixed pupil size: 11.0 mm diameter.

5.4. Comparison with perfect MTF

Our aim is to compare the experimental results with the theoretical calculations previously considered according to Eq (3) (see Fig 1). The MTFs corresponding to the He-Ne, semiconductor and laser pointers, and the perfect MTF have been jointly plotted in order to appreciate the differences arising for the contrast and cut-off frequency values (see Fig 7). The perfect MTF stands for the diffraction limit.

The data are represented in Fig (7a) in the range in which experimental MTFs are defined, up to 12.5 lines/mm. Figure (7b) displays the MTF curves for normalized spatial frequencies. We notice that the maximum cut-off spatial frequency stands for the laser semiconductor: the order of 12.5 lines/mm. However, no dramatic differences in spatial frequency values are observed, as determined by the degree of coherence

and diffraction limit of the optical system. Indeed, the differences between measured and perfect curves are around 17% and 44% at low and high spatial frequencies, respectively. Obviously, the experimental spatial frequency ranges for the three light sources are not comparable with the one for the perfect MTF. As a general data, the experimental curves have a frequency cut-off that is between 20% and 40% of the diffraction limit.

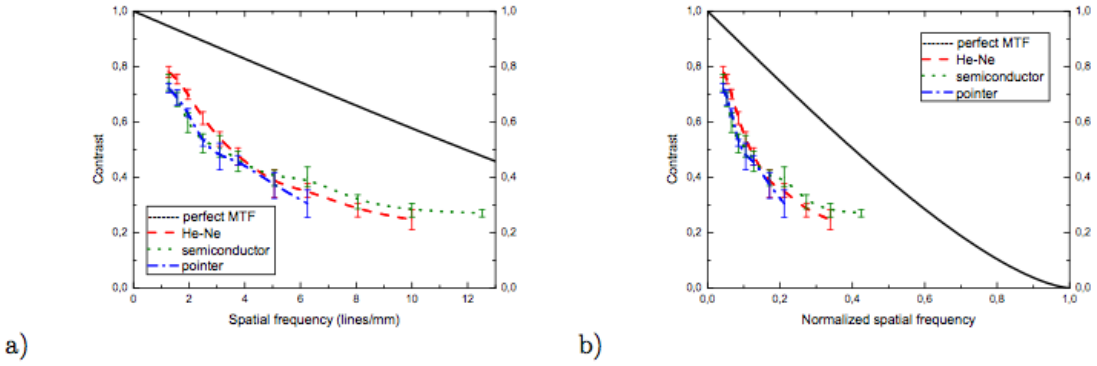

Fig 7. Average MTFs for three types of laser sources represented in: a) experimental scale, b) normalized spatial frequency scale. Solid line: Perfect MTF, diffraction limit; dashed line: He-Ne laser (λ= 655 nm) (LASING SL); dotted line: semiconductor laser (λ = 532 nm) (LASING SL); dashed-dotted line: pointer laser (λ = 402 nm) (LASING SL).

6 Discussion and conclusions

The performance of an optical image forming system with finite pupil has been evaluated by experimentally determining the MTF and merit functions. As a main objective, the design of the experimental setup pursues the simulation of the optical section of HVS. Also, the dependence of contrast on wavelength, spatial frequency and pupil size has been evaluated. The results show that the system operates in a standard fashion with expected results as predicted by MTF behavior in other studies. There are some restrictions to our model since real anatomy of human eye is not reproduced, thus the neural response is obviously not considered and as a consequence no data on the corresponding MTF have been handled. As facts, to be mentioned, there is a scale factor affecting real eye axial length and size of photoreceptors of a potential observer not reproduced here. Therefore, the influence of these factors on the performance of a visual test in real observes is not considered in the present study [20]. However, despite these limitations, the obtained and analyzed MTFs turn out to be characteristic ones of this type of experimental setups. The investigation can be extended to modified systems by real observers. Moreover, it is possible to study modified alternative tests and geometries. In the extended case of evaluating spatial frequency response in human eyes, both optical and neural responses need to be considered. And the experimental arrangement should be extended in order to obtain data with observers. As extended applications we can mention robotic vision displays.

Acknowledgements

Authors gratefully acknowledge the members of Optics Department of UCM who supplied invaluable advice: J A Rodrigo helped on the experimental setup; A V Velasco and T Alieva discussed the results and provided many suggestions. We are indebted to Prof P Artal and the Laboratory for Optics, Murcia University, for providing the necessary equipment to carry out the biometric measurements.

References

1. Goodman J W, Introduction to Fourier Optics, (Roberts & Company Publishers, Englewood, Colorado), 3rd edn, 2005.
. 2. Van der Lugt A B, Signal detection by complex spatial filtering, *IEEE Trans Inform Theory*, 10(1964)139–145.

3. Duffieux P M, L'Intégrale de Fourier et ses Applications à l'Optique, (Oberthur, Rennes), 1946 [in French]. Ibid, The Fourier Transform and its Applications to Optics, (Wiley, New York), 1983.
4. Ozhu H, Enoch J M, O'Hair J, Optical modulation by the isolated retina and retinal receptors, *Vision Res*, 12 (1972)231–244.
5. Williams T, The Optical Transfer Function of Imaging Systems, (Routledge, New York), 1999, Chapter 2. E book Published October 2017.
6. Yan Y, Thompson K, Burns S A, Pupil location under mesopic, photopic and pharmacologically dilated conditions, *Invest Ophthalmol Vis Sci*, 43(2002)2508–2512.
7. Atchison D A, Smith G, Optics of the Human Eye, (Butterworth-Heinemann, Edinburgh), 2002, 2nd edn, pp 23-25.
8. Lakshminarayanan V, Calvo M L, The optical transfer function and point spread function of the eye treated as a cascade linear system under Fresnel regime, Selected Topics in Mathematical Physics: Professor R Vasudevan Memorial Volume, eds Sridhar R, Srinivasa Rao K, Lakshminarayanan V, (Allied Publishers Pvt. Ltd.), 1995..
9. Campbell F W, Green D G, Optical and retinal factors affecting visual resolution, *J Physiol*, 181(1965)576–593.
10. Valois R De, Valois K De, Spatial Vision, (Oxford Science, New York), 1988, pp 157–160.
11. García-Guerra C E, Martínez-Roda J A, Aldaba M, Díaz-Doutón F, Vilaseca M, Vohnsen B, and Pujol J, Method to reduce undesired multiple fundus scattering effects in double-pass systems, *J Opt Soc Am A*, 36(2019)918–924.
12. Chung S T L, LaFrance M W, and Bedell H E, Influence of Motion Smear on Visual Acuity in Simulated Infantile Nystagmus, *Optom Vis Sci*, 88(2011)200–207.
13. Valente D, Vohnsen B, Retina-simulating phantom produced by photolithography, *Opt Lett*, 42(2017)4623–4626.
14. Artal P, Marcos S, Navarro R, Williams D R, Odd aberrations and double-pass measurements of retinal image quality, *J Opt Soc Am A*, 12(1995)195–201.
15. Calvo M L (Coord.), Optica Avanzada [Advanced Optics] (Ariel, Barcelona, 2007), Chapter 3: Optical Coherence [in Spanish].
16. Paredes-Barato D, Calvo M L, On the Thompson-Wolf experiment. A study with laser sources, *JEOS: Rapid Publications*, 5(2010)10051–10057.
17. Astadjov D N, Prakash O, Spatial coherence of low-cost 532nm green lasers, Proc SPIE, 8770, (2013) 87701P-1.
18. Alieva T, Calvo M L, Paraxial diffraction on structures generated by multiplicative iterative procedures, *J Opt A: Pure Appl Opt*, 5(2003)S324; doi.10.1088/1464-4258/5/5/386.
19. Watson A B, A formula for the mean human optical modulation transfer function as a function of pupil size, *J Vis*, 13(2013)18; doi. org/10.1167/13.6.18; and references therein..
20. Amorim A R, Bret B, González-Méijome J M, Opto-Mechanical Eye Models, a Review on Human Vision Applications and Perspectives for Use in Industry, *Sensors*, 22(2022)7686; doi.org/10.3390/s22197686.

[*Received*: 23.12.2022; *revised recd:*11.01.2023; *accepted*: 13.01.2023]

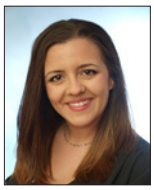

After her Bachelor degree in Physics at the Complutense University of Madrid (UCM, Spain), Elena Alonso enrolled in a Master degree on Biomedical Physics and she studied the modulation transfer function of an eye model, also at UCM. Afterwards, she moved to Mainz (Germany) and completed her Ph D on Brillouin scattering on soft matter at the Max Planck Institute for Polymer Science. Currently, Dr Alonso works as Communications Manager at IMDEA Nanociencia research institute in Madrid (Spain).